Geodesic Acoustic Modes in Multi-Ion System

Makoto SASAKI, Kimitaka ITOH[1)], Akira EJIRI[2)] and Yuichi TAKASE[2)]

Graduate School of Science, The University of Tokyo, Tokyo 113-0033, Japan
[1)]*National Institute for Fusion Science, Toki 509-5292, Japan*
[2)]*Graduate School of Frontier Sciences, The University of Tokyo, Kashiwa 277-8561, Japan*

(Received 2 November 2007 / Accepted 7 February 2008)

Geodesic acoustic modes (GAMs) in the multi-ion system are investigated. It was found that the high-frequency branch decreases with increase in effective ion mass. The low-frequency branch (ion sound wave, ISW) of the damping rate also becomes small. The ratio between the damping rate of GAM and ISW is found to become order of unity in the region of $q < 4$ (q is safety factor).

Keywords: geodesic acoustic mode, ion sound wave, multi-ion system, impurity

DOI: 10.1585/pfr.3.S1017

1. Introduction

Recently, the self-organizing meso-scale structure has attracted much attention. In particular, zonal flows (ZFs) are thought to reduce the anomalous transport driven by turbulence [1]. Geodesic acoustic modes (GAMs) [2], which are oscillatory modes, exists in toroidal plasmas. The study of GAMs is also essential for plasma research, because GAMs and ZFs share the energy generated from turbulence. The radial eigenmode of GAM is investigated [3–5]. In addition, a new diagnostic method, GAM spectroscopy, is proposed [6]. This method enables detection of the effective ion mass, which is equal to the abundance ratio of ions, by detecting radial eigenmodes of GAMs. It is important to investigate whether the method of GAM spectroscopy provides information of impurities. Thus, GAMs in multi-ion system are very important.

In this study, the GAMs frequencies in collisionless plasma with multiple ion species are investigated. The plasma is assumed to have a circular cross-section and a high aspect ratio. The analytical expression for frequency of GAM is derived. In addition, the lower-frequency branch, ion sound wave (ISW), is also analyzed. GAM frequency is found to become small with increase in effective ion mass. The damping rate of GAM becomes small around $q \sim 3$ (q is safety factor). In multi-ion systems, the damping rate of ISW is found to become small to such a degree that the ratio between the damping rates of ISW and GAM becomes of order of unity. This result indicates that ISW can be detected experimentally in the case that the energy generated in turbulence is injected to this branch as well as GAMs. The general formula of this study is explained in Section 2, the GAM and ISW branches are discussed in Sections 3 and 4, respectively, and a summary is given in Section 5.

author's e-mail: sasaki@fusion.k.u.tokyo.ac.jp

2. General Formula

The mathematical model is explained in this section. The magnetic field is assumed to be written as

$$\boldsymbol{B} = \frac{B_0}{1+\epsilon\cos\theta}\left(\boldsymbol{e}_\zeta + \frac{\epsilon}{q}\boldsymbol{e}_\theta\right), \tag{1}$$

where $\boldsymbol{e}_\theta$ and $\boldsymbol{e}_\zeta$ are poloidal and toroidal directions, and ϵ and q are the inverse aspect ratio and the safety factor, respectively. The basic equation, Gyrokinetic equation, and quasi-neutral condition can be written as

$$\left\{\frac{\partial}{\partial t} + v_\parallel \boldsymbol{b}\cdot\nabla + i\boldsymbol{k}_\perp\cdot\boldsymbol{v}_{\mathrm{dr}}\right\}\delta f^{(j)}_{k_\perp} = -\left\{v_\parallel \boldsymbol{b}\cdot\nabla + i\boldsymbol{k}_\perp\cdot\boldsymbol{v}_{\mathrm{dr}}\right\}\left(F^{(j)}_0 J_0(k_\perp\rho)\frac{e\phi_{k_\perp}}{T}\right), \tag{2}$$

$$\sum_j Z_j\int \mathrm{d}v^3\delta f^{(j)}_{k_\perp} - \sum_j Z_j n_j\left(1-\Gamma_0(k^2\rho_j^2/2)\right) \times \frac{e\phi_{k_\perp}}{T_\mathrm{i}} = \frac{n_\mathrm{e}}{T_\mathrm{e}}\left(\phi_{k_\perp} - <\phi_{k_\perp}>\right), \tag{3}$$

where $\delta f^{(j)}_{k_\perp}$ and $\phi_{k_\perp}$ are the response of distribution of jth ion and ZF potential, respectively. $Z_j, n_j, n_\mathrm{e}, T_\mathrm{i}$ and T_e are jth ion charge, density, ion temperature, electron density, and electron temperature, respectively. The angle brackets <> represent average over the magnetic surface. $F^{(j)}_0$ is Maxwell distribution, written as $F^{(j)}_0 = n_j/\pi^{3/2}\exp\left(-\hat{v}_j^2\right)$. $\hat{v}_j$ is the velocity normalized by jth ion thermal velocity. The thermal velocity can be written as $\hat{v}_j = \sqrt{T_\mathrm{i}/m_j}$. m_j is jth ion mass. Here, $\delta f^{(j)}_{k_\perp}$ and $\phi_{k_\perp}$ are expanded by Fourier series as

$$\delta f^{(j)}_{k_\perp} = \sum_{m=-\infty}^{\infty} e^{im\theta - i\omega t}\delta f^{(j)}_m(\omega), \tag{4}$$

$$\phi_{k_\perp} = \sum_{m=-\infty}^{\infty} e^{im\theta - i\omega t}\hat{\phi}_m(\omega). \tag{5}$$

Using Eqs. (2) and (3), the response of ions to the ZF potential is obtained as [7, 8]

$$i\hat{\omega}\delta f_0^{(j)} = \frac{1}{2}J_0\left(s\frac{\hat{v}_{\perp j}}{q}\right)k\hat{u}_j(\delta f_{-1}^{(j)} - \delta f_1^{(j)} + \hat{\phi}_{-1} - \hat{\phi}_1), \quad (6)$$

$$\delta f_m^{(j)} = \sum_{l,l'} J_0(s\hat{v}_{\perp j}/q)F_0\frac{\hat{v}_{\parallel j}(m-l)}{\omega - \hat{v}_{\parallel j}(m-l)}i^{l'-l} J_l(k\delta_1)J_{l'}(k\delta_1)\phi_{m-l-l'}, \quad (7)$$

where s_j is the finite orbit width, defined by $s_j = kv_jq/\Omega_j$. $\delta_j = -s_j\left(\hat{v}_{\parallel j} + \hat{v}_{\perp j}^2/2\hat{v}_{\parallel j}\right)$ represents the Doppler shift due to the toroidal effect. $\hat{\omega}_j = \omega R_0 q/v_j$ is the normalized frequency. Here, the poloidal harmonics are truncated, and the poloidal modes $m = 0, \pm 1$ are kept. The ion response can be written as

$$i\hat{\omega}\delta f_0^{(j)} = n_j\left(C_{00}^{(j)}\hat{\phi}_0 + C_{01}^{(j)}\hat{\phi}_1\right), \quad (8)$$

$$\delta f_1^{(j)} = n_j\left(C_{10}^{(j)}\hat{\phi}_0 + C_{11}^{(j)}\hat{\phi}_1\right). \quad (9)$$

C_{ij} is a coefficient, a function of velocity. Combining Eqs. (8) and (9) with the quasi-neutral condition Eq. (3), the dispersion relation is given by

$$\begin{aligned}\Delta = &\left\{\sum_j \frac{Z_j n_j}{n_e} i\frac{s_j^2}{2}\left[\frac{\hat{\omega}_j}{q^2} + \frac{1}{2}\right.\right.\\ &\left.\left.\times\left\{\frac{3}{2}\hat{\omega}_j + \hat{\omega}_j^3 + \left(\frac{1}{2} + \hat{\omega}_j^2 + \hat{\omega}_j^4\right)Z(\hat{\omega}_j)\right\}\right]\right\}\\ &\times\left\{\frac{1}{\tau_e} - \sum_j \frac{Z_j n_j}{n_e}\left(1 + \hat{\omega}_j Z(\hat{\omega}_j)\right)\right\}\\ &- \sum_j \frac{Z_j n_j}{n_e} s_j\left\{\hat{\omega}_j^2 + \left(\frac{1}{2}\hat{\omega}_j + \hat{\omega}_j^3\right)Z(\hat{\omega}_j)\right\}\\ &\times\sum_j \frac{Z_j n_j}{n_e} i\frac{s_j}{2}\left\{\hat{\omega}_j + \left(\hat{\omega}_j^2 + \frac{1}{2}\right)Z(\hat{\omega}_j)\right\}\\ &= 0. \end{aligned} \quad (10)$$

3. GAM Branch

The high-frequency branch, standard GAM is the solution derived under the assumption $\hat{\omega} > 1$. In this case, the plasma dispersion function $Z(\hat{\omega})$ can be expanded as

$$Z(\hat{\omega}) \approx -\left(\frac{1}{\hat{\omega}} + \frac{1}{2\hat{\omega}^3} + \frac{3}{4\hat{\omega}^5}\right) + i\sqrt{\pi}e^{-\hat{\omega}^2}. \quad (11)$$

The dispersion relation Eq. (10) can be expanded explicitly as

$$\Delta = A\hat{\omega} - (B + \delta B)\frac{1}{\hat{\omega}} - \frac{C}{\hat{\omega}^3} + i\left(De^{-\hat{\omega}^2} + Ee^{-\hat{\omega}^2/4}\right), \quad (12)$$

where $A,\ B,\ \delta B,\ C,\ D,\ E$ can be written as

$$A = \frac{1}{2q^2\tau_e}\sum_j \frac{Z_j n_j}{n_e}\left(\frac{Z_{main}}{Z_j\zeta_j}\right)^2\frac{1}{\zeta_j}, \quad (13)$$

$$B = \frac{7}{8\tau_e}\sum_j \frac{Z_j n_j}{n_e}\left(\frac{Z_{main}}{Z_j\zeta_j}\right)^2\zeta_j + \frac{1}{2}\sum_{j,j'}\frac{Z_j n_j}{n_e}\frac{Z_{main}}{Z_j\zeta_j}\frac{Z'_j n'_j}{n_e}\frac{Z_{main}}{Z'_j\zeta'_j}\zeta'_j, \quad (14)$$

$$\delta B = \frac{1}{4q^2}\sum_{j,j'}\frac{Z_j n_j}{n_e}\left(\frac{Z_{main}}{Z_j\zeta_j}\right)^2\frac{1}{\zeta_j}\times\frac{Z'_j n'_j}{n_e}\frac{Z_{main}}{Z'_j\zeta'_j}\zeta'^2_j, \quad (15)$$

$$\begin{aligned}C = &\frac{23}{16\tau_e}\sum_j \frac{Z_j n_j}{n_e}\left(\frac{Z_{main}}{Z_j\zeta_j}\right)^2\zeta_j^3\\ &-\frac{7}{16}\sum_{j,j'}\frac{Z_j n_j}{n_e}\left(\frac{Z_{main}}{Z_j\zeta_j}\right)^2\zeta\frac{Z'_j n'_j}{n_e}\zeta'^2_j\\ &+\frac{1}{2}\sum_{j,j'}\frac{Z_j n_j}{n_e}\frac{Z_{main}}{Z_j\zeta_j}\frac{Z'_j n'_j}{n_e}\frac{Z_{main}}{Z'_j\zeta'_j}\\ &\times\left(\zeta'^3_j + \zeta_j^2\zeta'_j\right),\end{aligned} \quad (16)$$

$$D = \sqrt{\pi}\frac{Z_{main}n_{main}}{n_e}\frac{1}{2\tau_e}\hat{\omega}^4 + \left\{\frac{1}{2} - \frac{\tau_e}{4}\sum_j \frac{Z_j n_j}{n_e}\zeta_j^2 + \frac{\tau_e}{2}\frac{Z_j n_j}{n_e}\frac{Z_{main}}{Z_j\zeta_j} + \frac{\tau_e}{2}\frac{Z_j n_j}{n_e}\frac{Z_{main}}{Z_j}\right\}\hat{\omega_G}^2, \quad (17)$$

$$E = \sqrt{\pi}\frac{Z_{main}n_{main}}{n_e}\frac{1}{2\tau_e}\frac{\hat{\omega}^6}{1024}, \quad (18)$$

$$\zeta_j = \sqrt{\frac{m_{main}}{m_j}\tau_j}, \quad (19)$$

where ζ_j is the thermal velocity ratio, τ_j is the j ion temperature normalized by main ion temperature $\tau_j = T_j/T_{main}$. m_{main}, Z_{main} and n_{main} are the mass, charge, and density of main ion. The solution of this dispersion relation can be obtained as

$$\omega_G = \frac{v_T}{R_0 q}\frac{B}{A}\left\{1 + \left(\frac{B\delta B}{A^2} + \frac{C}{A}\right)\frac{B}{A}\right\}, \quad (20)$$

$$\begin{aligned}\gamma_G \approx &-\sqrt{\pi}\frac{Z_{main}n_{main}}{n_e}q\frac{v_T}{R_0}\left\{\sum_j \frac{Z_j n_j}{n_e}\left(\frac{Z_{main}}{Z_j\zeta_j}\right)^2\right.\\ &\left.\times\frac{1}{\zeta_j}\right\}^{-1}\left[\left\{\frac{\hat{\omega_G}^4}{2} + \left\{\frac{1}{2} - \frac{\tau_e}{4}\sum_j \frac{Z_j n_j}{n_e}\zeta_j^2\right.\right.\right.\\ &\left.+\frac{\tau_e}{2}\frac{Z_j n_j}{n_e}\frac{Z_{main}}{Z_j\zeta_j} + \frac{\tau_e}{2}\frac{Z_j n_j}{n_e}\frac{Z_{main}}{Z_j}\right\}\\ &\left.\left.\times\hat{\omega_G}^2\right\}e^{-\hat{\omega_G}^2} + s^2\frac{\hat{\omega_G}^6}{1024}e^{-\hat{\omega_G}^2/4}\right].\end{aligned} \quad (21)$$

The real frequency ω_G agrees with the result of [8, 9] in the limit of single-ion $\sum_j Z_j n_j \rightarrow n_{main}$. In the limit of $\sum_j Z_j n_j \rightarrow Z_1 n_1$, which is the impurity limit, ω_G becomes

$$\omega_G \rightarrow \zeta\omega_{G0}\left(1 + \frac{\zeta}{Z_1}\frac{\alpha}{q^2}\right), \quad (22)$$

where $\omega_{G0} = v_T/R_0\sqrt{7/4+\tau_e}$, $\alpha = (23+16\tau_e+4\tau_e^2)/(7+4\tau_e)^2$. The frequency of the leading order becomes approximately ζ times small compared with that for hydrogen plasma. The higher-order term of the $1/q^2$ order becomes ζ/Z_1 times small. The result of the real frequency in a two-ion system is shown in Fig. 1, which is obtained from Eq. (20). The real frequency depends on the thermal velocity, as seen in Eq. (20). In the multi-ion system, the effective mass becomes larger than in the single-ion case; therefore, the effective thermal velocity becomes small. For this reason, the GAM real frequency becomes small with the increase in the number of heavier ions. The q dependence of the real frequency is shown in Fig. 2. The normalized real frequency has the tendency of linearly increasing with q. The behavior of the damping rate is shown in Fig. 3 in the case of $Z_{\mathrm{eff}} = 4$, as obtained from Eq. (10) numerically. Here, the effective charge Z_{eff} is defined by $Z_{\mathrm{eff}} = \sum_j Z_j^2 n_j / \sum_j Z_j n_j$. The damping rate in multi-ion systems is found to be larger. In particular, the damping rate becomes smaller around $q \sim 3$, 4, because the terms related to $e^{-\omega_G^2/4}$ becomes effective.

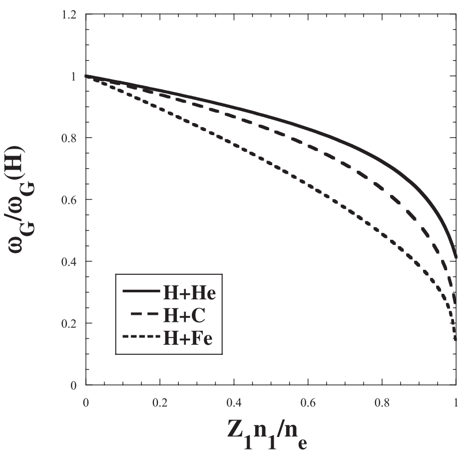

Fig. 1 Multi-ion effect on GAM real frequency.

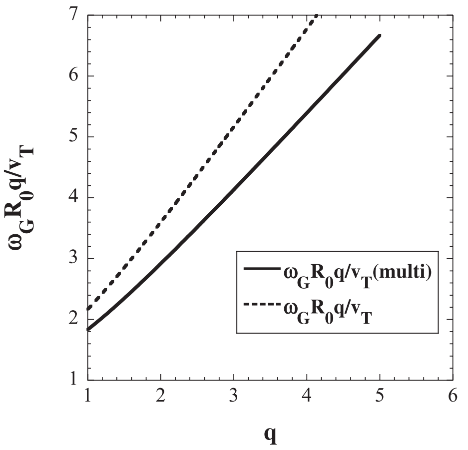

Fig. 2 Dependency of GAM real frequency.

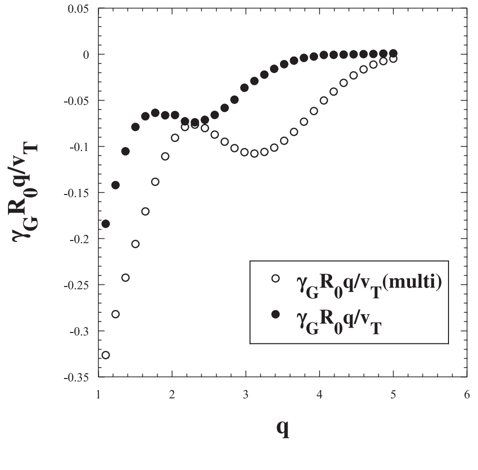

Fig. 3 Multi-ion effect on GAM damping rate. Ions consist of hydrogen and carbon. $Z_{\mathrm{eff}} = 4$.

4. ISW Branch

The dispersion relation Eq. (10) also gives solutions other than GAM, such as a low-frequency mode (LFM) and ISWs. LFM has the zero frequency and a finite damping rate, and ISWs are solutions other than GAM and LFM, and exist in both low- and high-frequency regions. ISWs in the high-frequency region have much larger damping rates than GAM, because they are strongly damped by Landau damping. Therefore, in this study, we pay attention to the modes in the low-frequency region. In particular, we analyze the mode whose damping rate is the smallest among them. The numerical solutions of ISWs and LFM are obtained by Eq. (10).

The behavior of the modes in the low-frequency region is shown in Fig. 4. First, in the case of a single-ion system, the LFM damping rate is smaller than that of ISW in the region of $q < 2$, and becomes larger in the region of $q > 2$. This means that it is easier to experimentally detect LFM in $q < 2$ and ISW in $q > 2$. Second, in the case of a multi-ion system, the damping rate of LFM is smaller in

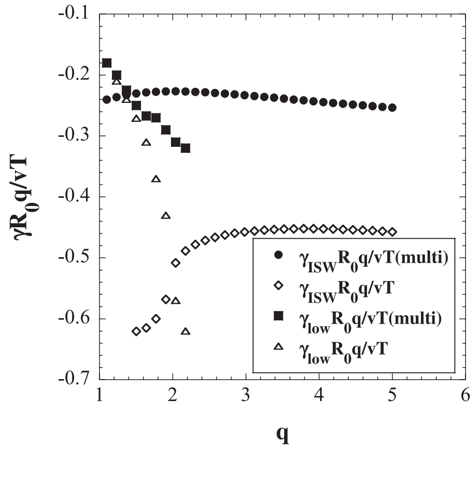

Fig. 4 Comparison between damping rate of ISW in multi-ion and single-ion systems.

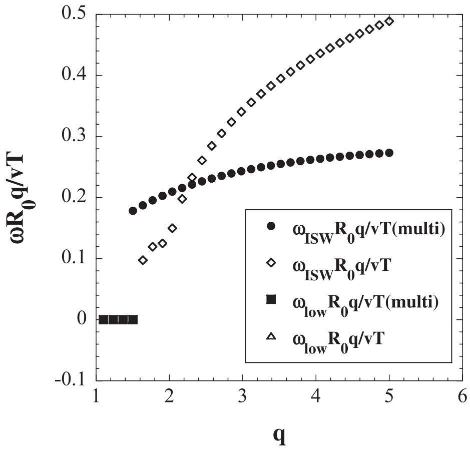

Fig. 5 Comparison between real frequency of ISW in multi-ion (hydrogen and carbon; $Z_{\mathrm{eff}} = 4$) and single-ion systems.

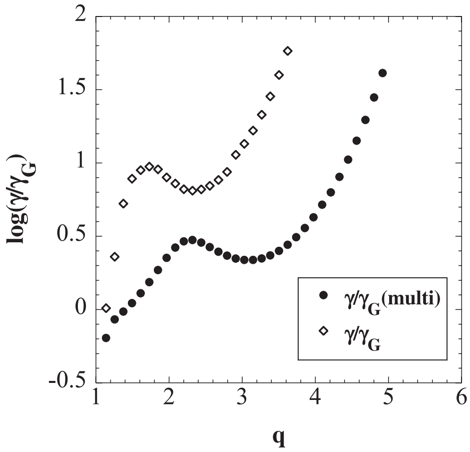

Fig. 6 Ratio between damping rates of ISW and GAM.

the region of $q < 1.5$, and becomes larger in the region of $q > 1.5$. By comparing the two systems, it is found that the damping rate of the multi-ion case becomes much smaller than in the single-ion case in the region of $q > 2$.

The behavior of the real frequency, whose damping rate is the smallest, is shown in Fig. 5. The frequencies jump at $q \sim 2$ in the single-ion case, and at $q \sim 1.5$ in the multi-ion case, because the mode whose damping rate is the smallest changes from LFM to ISW with increase in q.

The ratio of damping rates of ISW (including LFM) and GAM is found to become of the order of unity, as shown in Fig. 6. This result indicates that ISW can be observed experimentally.

5. Summary

GAMs in multi-ion system were investigated in the collisionless limit. The plasma is assumed to have a circular cross-section, and high aspect ratio. The high-frequency branch, standard GAM, is analyzed. The analytic expression for frequency is obtained. With increase in effective ion mass, GAM frequency decreases. These results are essential for GAM spectroscopy. The damping rate of standard GAM becomes smaller than the single-ion system. This influences the energy partition between ZFs and GAMs. In addition, the low-frequency branch, ISW and LFM, is analyzed. The damping rate in multi-ion systems becomes small, and their damping rates become comparable. Thus, if the turbulent energy is injected into this branch, this mode can be observed experimentally.

[1] P.H. Diamond, S.-I. Itoh, K. Itoh and T.S. Hahm, Plasma Phys. Control. Fusion **47**, R35 (2005).

[2] N. Winsor, J.L. Johnson and J.J. Dawson, Phys. Fluids **11**, 2248 (1968).

[3] T. Ido, Y. Miura, K. Hoshino, K. Kamiya, Y. Hamada, A. Nishizawa, Y. Kausumi, H. Ogawa, Y. Nagashima, K.S hinohara, Y. Kusama and JFT-2 M group, Nucl. Fusion **46**, 512 (2006).

[4] K. Itoh, S.-I. Itoh, P.H. Diamond, A. Fujisawa, M. Yagi, T. Watari, Y. Nagashima and A. Fukuyama, Plasma Fusion Res. **1**, 037 (2006).

[5] M. Sasaki, K. Itoh, A. Ejiri and Y. Takase, Contrib. Plasma Phys. **48**, 68 (2008).

[6] S-I. Itoh, K. Itoh, M. Sasaki, A. Fujisawa, T. Ido and Y. Nagashima, Plasma Phys. Control. Fusion **49**, L7-L10 (2007).

[7] Zhe. Gao, K. Itoh, H. Sanuki and J.Q. Dong, Phys. Plasmas **13**, 100702 (2006).

[8] H. Sugama and T.-H. Watanabe, J. Plasma. Phys. **72**, 825 (2006).

[9] M. Sasaki, K. Itoh, A. Ejiri and Y. Takase, Plasma Fusion Res. **3**, 009 (2008).